

THERMAL EVOLUTION OF FLUORINE FROM SMECTITE AND KAOLINITE

STEVE J. CHIPERA* AND DAVID L. BISH

Earth and Environmental Sciences Division, Los Alamos National Laboratory, Mail Stop D469, Los Alamos, New Mexico 87545, USA

Abstract—The fluoride ion is crystal chemically very similar to the hydroxyl ion, substituting for hydroxyl in many minerals in which hydrogen bonding is not important. Fluoride substitutions are particularly common in 2:1 layer silicates, such as micas, illites and smectites. The brick and tile industries, which use naturally occurring clays as their primary raw materials, have devoted considerable effort to understanding fluorine evolution during firing of the raw materials due to increasingly stringent fluorine emission regulations. In order to understand fluorine evolution from ceramic raw materials, we have studied a number of phyllosilicate materials used in making bricks. X-ray powder diffraction and fluorine analyses were combined with heating experiments and thermogravimetric analysis to evaluate the chemical and structural changes taking place on heating. Fluorine remained in 2:1 layer silicates to higher temperatures than did hydroxyl, but it behaved identically to hydroxyl in the kaolinite studied. In all cases, fluorine evolution coincided with structural breakdown of the clay host. These results show that fluorine evolution will consistently occur during firing of clay raw materials, and the problems of fluorine emission cannot be readily solved by simple variations of firing temperatures or times.

Key Words—Brick, Firing, Fluorine, Kaolinite, Smectite, TGA, Thermogravimetric Analysis, X-ray Diffraction.

INTRODUCTION

The occurrence and importance of fluorine in geological materials has been recognized since the early part of the last century (*e.g.* Steinkoenig, 1919; Clarke and Washington, 1924). However, as a result of the difficulty in analyzing for fluorine using traditional analytical techniques, standard analyses of geological materials have rarely included fluorine. With the introduction of the F⁻-selective electrode and ion chromatography, analysis for fluorine became straightforward, and the occurrence of fluorine in geological materials has since become better documented (*e.g.* Ingram, 1970; Troll *et al.*, 1977; Keller, 1986).

In one of the first comprehensive studies of fluorine in geological materials, Robinson and Edgington (1946) measured the fluorine content of 137 soil samples. Although a significant amount of literature existed at that time on biological aspects of fluorine, few data existed on the fluorine content of soils. Robinson and Edgington concluded that, in general, the main source of fluorine in ordinary soils was micaceous clays. Thomas *et al.* (1977) found that fluorine varied among the various clay mineral groups; they postulated that the amount of fluorine in a sample is dependent on the amount of fluorine in the environment during the mineral's formation or in the groundwater surrounding the mineral, depending on the mineral's ability to exchange F⁻ for OH⁻. They suggested that fluorine

might be a potentially important geochemical indicator of the origin and depositional environment of clays and shales.

Bassett (1960) was perhaps the first to suggest that the relative stability of dioctahedral and trioctahedral micas is linked to the orientation of their structural hydroxyl groups. He hypothesized that dioctahedral micas are less susceptible to alteration because their inclined hydroxyl groups result in an energetically more favorable environment for the interlayer potassium ion. The hydroxyl group in trioctahedral micas is approximately perpendicular to the layers, maximizing the repulsive electrostatic interaction between the hydroxyl proton and the interlayer potassium ion. Giese (1978) used electrostatic energy calculations to confirm that the orientation of hydroxyl groups in phyllosilicates is crucial in determining interlayer bonding energy. Giese (1975) also showed that the fluorine content of phyllosilicates is often directly linked with the details of the crystal structure. For example, as a result of proton-potassium interactions, fluoride substitutions for hydroxyl are more energetically favorable in a trioctahedral mica than in a dioctahedral mica. Giese (1982) showed that fluoride-for-hydroxyl substitution in kaolinite markedly destabilizes the structure, a reflection of the importance of interlayer hydrogen bonding in the kaolin minerals. On the basis of these modeling studies, one would expect trioctahedral 2:1 layer silicates to be enriched in fluorine relative to dioctahedral minerals. Likewise, it might be expected that kaolin minerals would contain little fluoride in their interlayer hydroxyl sites. A recent ¹⁹F nuclear magnetic resonance study (Labouriau *et al.*, 1995) could not distinguish between

* E-mail of address corresponding author:
Chipera@lanl.gov

fluoride in interlayer and inner hydroxyl sites in kaolinite, suggesting either that fluoride in both types of sites is energetically indistinguishable or that fluoride is present in only one type of site.

As a result of increasingly stringent environmental regulations, brick and tile manufactures have become concerned with fluorine emissions during the firing process (*e.g.* Wilson and Johnson, 1975; Strohmenger, 1983; Kolkmeier, 1986; Sedej, 1988). In addition, fluorides are known to be among the most poisonous industrial pollutants (Sedej, 1988). Plants that are subjected to fluorides do not show effects immediately, and only after they have accumulated a certain plant-dependent threshold level do they exhibit the effects of fluorine toxicity. Consumption of these plants by people or animals can then cause various diseases usually associated with bone or bone tissue (Eagers, 1969; Sedej, 1988).

Hauck and Hilker (1986) concluded that there are in principle only two methods available to reduce the fluorine concentrations associated with the flue gases from brick and tile manufacturing plants. The first is to remove the fluorine from the flue gases using cleaning or scrubbing devices. The second is to decrease the fluorine emission from the brick materials by changing the firing process or by influencing the composition of the raw clay materials. If fluorine emissions are to be reduced using the latter method, it is essential to obtain a better understanding of the nature of fluorine within the raw materials and how fluorine evolves during the firing process. This study examines the thermal behavior of fluorine in the smectite- and kaolin-group minerals, two of the most common clay groups used in the production of bricks.

MATERIALS AND METHODS

Brick raw materials used in this study were provided by the Texas Mining & Reclamation Association, a consortium of Texas brick manufacturers representing the Acme, Athens and Elgin-Butler Brick Companies. Analyses were conducted to determine the mineralogy and fluorine abundance of all of the materials. A 0.10–0.35 μm particle size-fraction of Acme Brick Company's Chew clay was chosen for study as representative of the smectite-group minerals used in the raw brick materials. This clay is from a Pleistocene oxbow lake deposit in Austin County, Texas, and consists mainly of a partially R1-ordered dioctahedral illite-smectite (I-S) with ~40% collapsed layers, with minor amounts of kaolinite and illite (Chipera and Bish, 1989). Sample API#9 from Mesa Alta, New Mexico (Kerr and Kulp, 1949), was chosen to provide information on fluorine in kaolin-group minerals. The kaolinite is well ordered and contains only trace impurities of quartz and anatase (Bish *et al.*, 1999). During the course of this study, hectorite (SHCa-1), a fluorine-, Li-rich

smectite, was also investigated to determine whether fluorine has a significant effect on the thermal behavior of smectite.

X-ray powder diffraction (XRD) was used to determine the mineralogical composition of the various samples and to monitor structural breakdown during heating. XRD analyses were obtained on an automated Siemens D-500 powder diffractometer, using $\text{CuK}\alpha$ radiation, incident- and diffracted-beam Soller slits, and a solid-state Si(Li) detector. Data were collected from 2° to $70^\circ 2\theta$, with a step size of $0.02^\circ 2\theta$ using count times of at least 2 s per step. Bulk samples were ground under acetone in a Brinkmann Micro Rapid mill to produce a powder with an average particle size of $<3 \mu\text{m}$ as confirmed using an Horiba CAPA 500 particle size distribution analyzer calibrated using Duke Scientific glass microspheres. The XRD mounts were prepared by pressing the powders into a machined cavity in a glass plate. Several clays were sedimented onto off-axis-cut quartz plates to obtain diffraction patterns of oriented clay-aggregate samples. The XRD data were analyzed using the Siemens DIFFRAC5000 software package, and quantitative XRD analyses were conducted using the external standard or 'adiabatic' method of Chung (1974). Interpretation of I-S interstratification was facilitated through comparisons of the observed (oriented clay aggregate) XRD patterns with patterns calculated using the program NEWMOD (Reynolds and Reynolds, 1987).

Clay extraction and purification of the Texas brick materials and of hectorite (which contains significant calcite) were accomplished by suspending the samples in deionized water, disaggregating them with a Braun-sonic 1510 ultrasonic probe for 10 min at 200 W, and applying Stokes' law of settling to obtain various size fractions (Chipera *et al.*, 1993). The purity of the various size-fractions was determined using XRD.

Fluoride ion analyses were obtained with a Dionex 4500i ion chromatograph. Thermogravimetric analyses (TGA) were performed on a PL Thermal TGA-1000, calibrated using Curie-point temperature standards, and analyses were run from 23 to 900 or 950°C at a rate of 10°C/min using dry nitrogen as a carrier gas. Additionally, hectorite was run from 23 to 1000°C at a rate of 2°C/min to better define weight losses.

To study the evolution of fluorine from the three clay materials, ~5 g of each clay were placed into ceramic crucibles and were heated at respective temperatures for ~16 h in a furnace calibrated to NIST-traceable standards. At each temperature of interest, ~200 mg aliquots of the clays were removed for XRD analysis and ion chromatography. The remaining sample was then heated at the next temperature step. Using this procedure, fluorine evolution was monitored by analyzing the heated residue rather than by analyzing the evolved gases as has been done in other studies (*e.g.* Hauck and Hilker, 1986). During the heating of the Chew I-S, a control crucible of the clay was weighed at each

Table 1. Quantitative mineral analyses of Texas brick samples.

Sample	Smectite	Mica	Kaolinite	Illite	Chlorite	Quartz	Calcite	Feldspar	Anatase	F ⁻ (ppm)
ACME Brick Company										
Texas Plant										
Abel Sand	6 ± 2	Trace	8 ± 2	–	–	85 ± 8	1 ± 1	–	–	n/a
Chew Clay (bulk material)	38 ± 15	–	7 ± 3	4 ± 1	–	27 ± 5	24 ± 5	Trace	–	671
>3.0 μm fraction	n/a	n/a	n/a	n/a	n/a	n/a	n/a	n/a	n/a	236
3.0–0.35 μm fraction	31 ± 12	–	7 ± 3	11 ± 4	–	25 ± 5	25 ± 5	1 ± 1	–	535
0.35–0.1 μm fraction	79 ± 43	–	6 ± 2	14 ± 7	–	1 ± 1	Trace	–	–	1032
Tulsa, Oklahoma, Plant										
Body Mix (bulk material)	–	–	–	42 ± 19	7 ± 2	39 ± 7	1 ± 1	11 ± 2	–	651
50–3.0 μm fraction	–	–	–	22 ± 9	3 ± 1	59 ± 8	1 ± 1	14 ± 3	–	186
<3.0 μm fraction	–	–	–	62 ± 29	8 ± 3	21 ± 6	Trace	8 ± 3	–	776
Malvern, Arkansas, Plant										
Ground Mix (bulk material)	4 ± 1	–	4 ± 1	20 ± 7	–	71 ± 9	–	1 ± 1	–	308
10.0–3.0 μm fraction	7 ± 3	–	16 ± 6	25 ± 10	–	51 ± 8	–	Trace	–	324
3.0–0.35 μm fraction	26 ± 12	–	63 ± 24	Trace	–	12 ± 3	–	–	–	318
ATHENS Brick Company										
Crowder	4 ± 2	Trace	69 ± 27	–	–	27 ± 6	–	–	–	150
Cumbie Sand	Trace	1 ± 1	21 ± 6	–	–	78 ± 9	–	Trace	–	<10
Harbinson-Walker	1 ± 1	Trace	76 ± 30	–	–	21 ± 6	–	–	–	186
McGlaun	8 ± 3	Trace	35 ± 11	–	–	57 ± 8	–	–	Trace	14
ELGIN-BUTLER Brick Company										
Buff	10 ± 4	1 ± 1	38 ± 13	–	–	51 ± 8	–	–	1 ± 1	250
Calcine	14 ± 5	1 ± 1	–	–	–	85 ± 9	–	–	1 ± 1	130
Sand	–	–	Trace	–	–	99 ± 10	–	1 ± 1	–	n/a
Elstan (bulk material)	30 ± 12	1 ± 1	11 ± 3	–	–	49 ± 7	–	9 ± 2	–	208
>50 μm fraction	14 ± 5	1 ± 1	1 ± 1	–	–	79 ± 9	Trace	5 ± 1	–	194
50–3.0 μm fraction	28 ± 10	2 ± 1	8 ± 3	–	–	55 ± 8	–	8 ± 2	–	483
3.0–0.35 μm fraction	83 ± 46	1 ± 1	10 ± 5	–	–	6 ± 3	–	–	–	782
0.35–0.1 μm fraction	82 ± 46	–	17 ± 8	–	–	1 ± 1	–	–	–	657

Trace = trace abundance <0.5 wt.%

n/a = not analyzed

– = not detected

temperature to determine the weight-loss behavior of the sample during long-term heating.

RESULTS AND DISCUSSION

Initial investigations of the Texas brick materials were conducted by optimizing XRD run conditions (long count times over primary diffraction peaks) for detection of trace amounts of potential fluorine-bearing phases (e.g. fluorite – CaF₂). No fluorine-bearing minerals were detected (at levels of ~0.1%), suggesting that fluorine resided in the clay minerals rather than in trace phases. This hypothesis was supported by chemical analysis of several purified clays obtained from the brick raw materials and by heating experiments. The mineralogy and fluorine contents of the Texas brick samples are shown in Table 1. The samples contain varying amounts of clay minerals consisting mainly of smectite, illite, kaolinite and mica, although the samples from Acme, Tulsa, Oklahoma, also contain chlorite. Other minerals present include quartz, feldspar, calcite and anatase. The errors reported in Table 1 represent estimated 2σ values.

Statistical analyses show that the fluorine contents in the brick raw materials correlate directly with the abundance of 2:1 layer-silicate minerals ($r = 0.92$, Figure 1). Although the fluorine contents generally decrease as the abundance of kaolinite increases, the relationship is not statistically significant ($r = -0.45$).

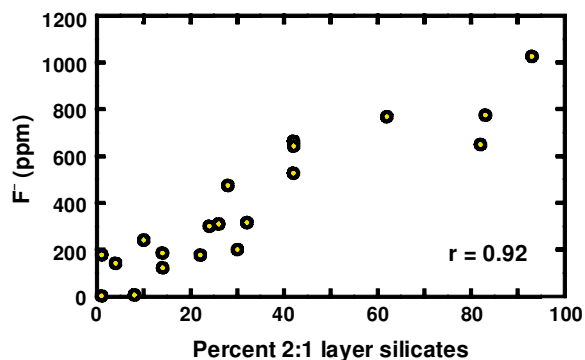


Figure 1. Percentage of 2:1 layer silicates (smectite, mica, illite) vs. fluorine (ppm) for the Texas brick raw materials listed in Table 1.

Evolution of fluorine from I-S and smectite-group minerals

Thermogravimetric analysis (TGA) (Figure 2) of the Acme Chew I-S showed that volatile evolution occurred in four distinct steps. The first corresponds to the loss of interlayer water (outer hydration shell) at $\sim 71^\circ\text{C}$ and the second corresponds to the loss of the remaining interlayer water at $\sim 136^\circ\text{C}$. The combined interlayer water loss represents a reduction of ~ 9.2 wt.%. The third and fourth weight-loss events correspond to dehydroxylation of the I-S, occurring from 350 to $\sim 650^\circ\text{C}$ and yielding an additional loss of ~ 6 wt.%. It is noteworthy that chemical analyses of heated aliquots from 16 h step heating of the Chew I-S showed that fluorine (which occupies only $\sim 1.5\%$ of the hydroxyl sites) remained in the sample to temperatures greater than those at which water and most hydroxyl were released (Figure 3a). Fluorine evolved from the Chew I-S at temperatures from ~ 600 to 750°C . Based on XRD monitoring of the integrated intensity of the 001 reflection, no evidence for destruction of the clay structure was apparent until above 700°C , with destruction becoming more rapid at 760°C , just after evolution of the fluorine (Figure 3b). With continued heating, the I-S structure was completely destroyed by 840°C , and the material remained relatively X-ray amorphous until ~ 950 – 1000°C , when spinel, hematite and cristobalite formed. The control crucible containing Chew I-S, weighed after each 16 h step heating (Figure 3c), showed weight-loss characteristics similar to the TGA analyses (Figure 2), with the following exceptions. First, because data were collected in 50 – 100°C increments, the 16 h heatings did not have the resolution of the TGA analyses. Second, it appears that dehydroxylation occurred at slightly lower temperatures in the 16 h heatings, which was expected because

the 16 h heatings allowed more time for equilibration, thereby minimizing kinetic effects that are common with more rapid heating.

The TGA analysis of the hectorite (Figure 4) showed that volatile evolution occurred in several less distinct steps. The first, which peaked at $\sim 47^\circ\text{C}$, corresponds to the loss of interlayer water. After the initial loss of interlayer water, weight loss was gradual until becoming more rapid at $\sim 700^\circ\text{C}$. The gradual weight loss is probably attributable to dehydroxylation. The more rapid weight loss from $\sim 700^\circ\text{C}$ to $>1000^\circ\text{C}$ is attributed to the loss of both fluorine (which occupies $\sim 1/3$ of the hydroxyl/fluoride sites) and the remaining hydroxyl during the thermal destruction of the hectorite. Chemical analyses of heated aliquots from 16 h step-wise heating of the hectorite showed that the fluorine remained in the structure until $\sim 650^\circ\text{C}$ whereupon it evolved rapidly until $\sim 850^\circ\text{C}$ where only $\sim 3\%$ of the original fluorine remained (Figure 5a). Based on XRD monitoring of the integrated intensity of the 001 reflection, no evidence for destruction of the clay structure was observed until ~ 650 – 700°C . The exact point of structure destruction is difficult to determine due to the variation in intensities as a result of different amounts of preferred orientation in the sample mounts (Figure 5b), but the hectorite 001 reflection was not detectable at $\sim 840^\circ\text{C}$. Unlike the results for the Chew I-S, fluorine evolution from hectorite started and ended at slightly higher temperatures than those where structural breakdown started and terminated.

Because fluorine evolved at temperatures higher than those required for dehydroxylation, fluoride appears to be stabilized in these structures relative to hydroxyl. Interestingly, the structure of hectorite, a trioctahedral smectite, broke down at approximately the same temperature as the Chew I-S. However, unlike the

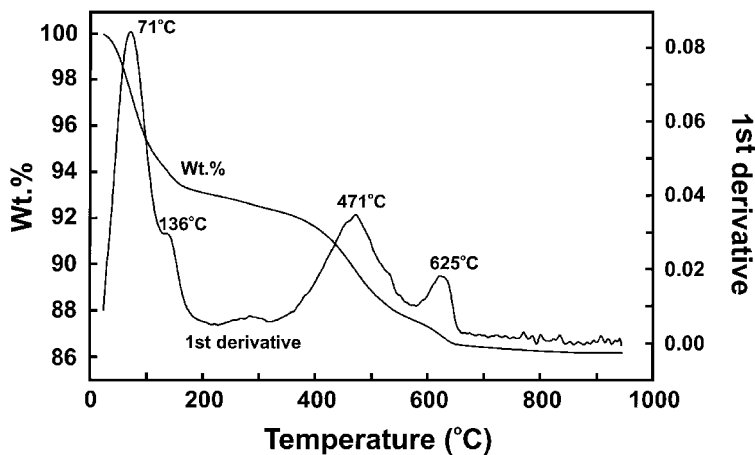


Figure 2. TGA analysis of the Chew I-S. The weight loss peaking at $\sim 71^\circ\text{C}$ corresponds to the evolution of interlayer water (outer hydration shell); the weight loss peaking at $\sim 136^\circ\text{C}$ corresponds to evolution of the remaining interlayer water, and the weight losses peaking at ~ 471 and 625°C correspond to smectite dehydroxylation. Fluoride occupies $\sim 1.5\%$ of the hydroxyl sites and evolves at the latest stage of dehydroxylation.

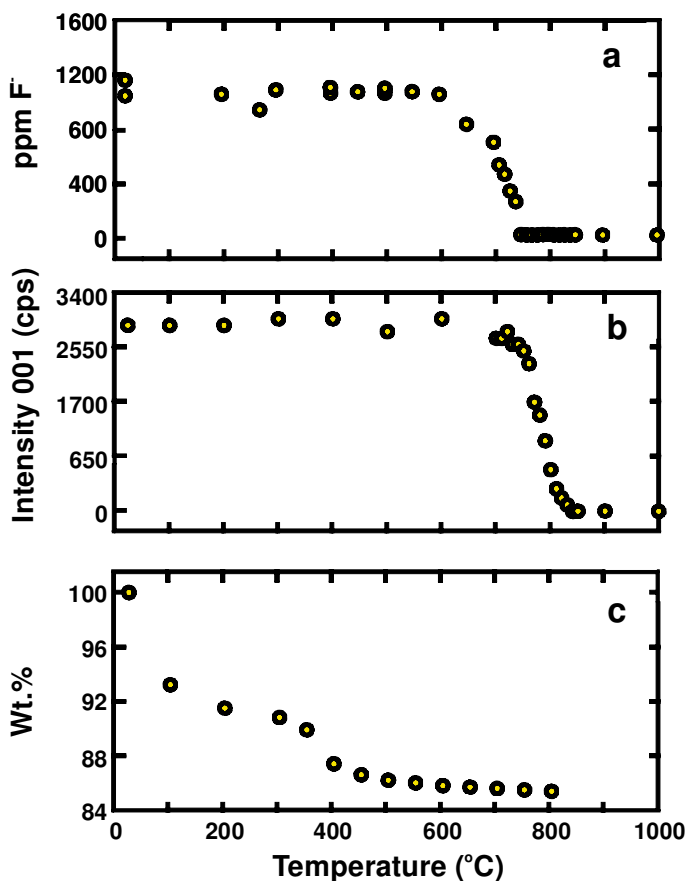


Figure 3. Stepwise 16 h heatings of the Acme Chew I-S. (a) Fluorine content (ppm) as a function of temperature. Fluorine began to evolve at $\sim 600^{\circ}\text{C}$ and terminated at 750°C . (b) Integrated intensity of the 001 reflection as a function of temperature showing that the structure began to break down above 700° and was completely destroyed at 840°C . (c) Weight loss measured from the 16 h step-wise heatings of the control crucible.

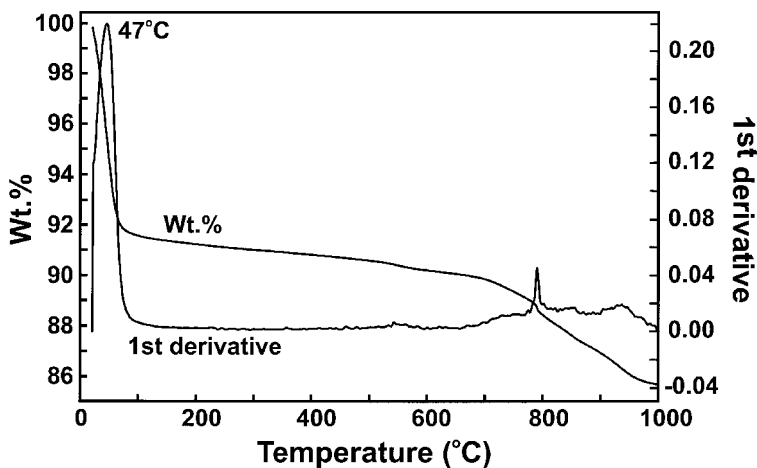


Figure 4. TGA analysis of the SHCa-1 hectorite. The weight loss peaking at $\sim 47^{\circ}\text{C}$ corresponds to the evolution of interlayer water. The gradual weight loss from 100 to 700°C probably represents dehydroxylation; the more rapid weight loss from 700 to 1000°C , which corresponds to the structural breakdown of the clay, probably represents the evolution of fluorine and any remaining hydroxyl. Fluoride occupies approximately one third of the hydroxyl sites in this sample.

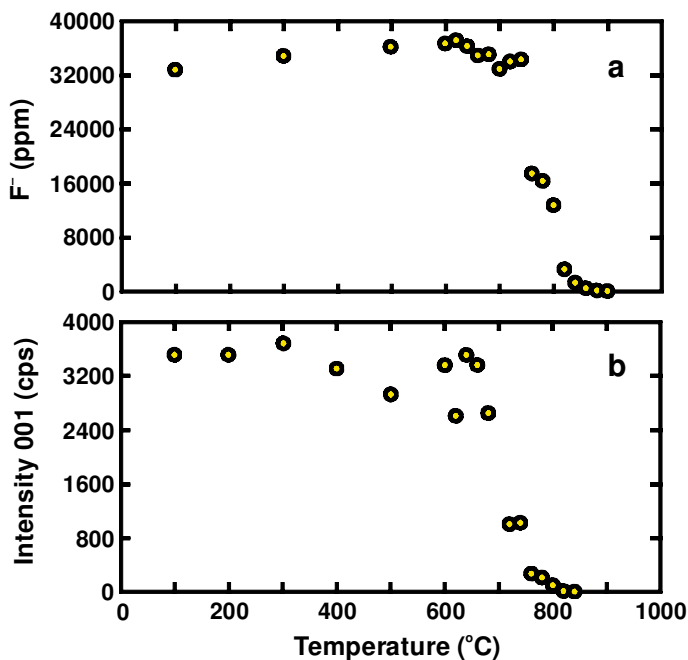


Figure 5. Stepwise 16 h heatings of the SHCa-1 hectorite. (a) Fluorine content (ppm) as a function of temperature. Fluorine began to evolve at $\sim 650^{\circ}\text{C}$ and terminated at $\sim 850^{\circ}\text{C}$. (b) Integrated intensity of the 001 reflection as a function of temperature showing that the structure began to break down after $\sim 700^{\circ}\text{C}$ and was completely destroyed at 840°C .

Chew I-S, fluorine remained in the hectorite structure to temperatures higher than the breakdown temperature.

It is well known that fluorine increases the thermal stability of trioctahedral 2:1 layer silicates such as micas (*e.g.* Romo and Roy, 1957; Sugiyama *et al.*, 1988). As noted above, several authors (*e.g.* Giese, 1975) have suggested, and electrostatic energy calculations have demonstrated, that the hydroxyl proton exerts a destabilizing influence on the structure due to electrostatic repulsion between the proton and the interlayer cation, an interaction which is absent when fluoride replaces hydroxyl. Our results show, however, that fluorine does not significantly increase the thermal stability of the dioctahedral Chew I-S. These results are consistent with electrostatic energy calculations of Giese (1975) that show significant energy stabilization resulting from fluoride-for-hydroxyl substitution in trioctahedral 2:1 layer silicates, but only a minor stabilization in dioctahedral 2:1 layer silicates.

In an attempt to evaluate the energetic effects of fluoride-for-hydroxyl substitution in layer silicates, we performed a number of electrostatic energy calculations for muscovite and phlogopite using the program ELEN (Ohashi and Burnham, 1972). Substitution of F for OH was modeled by replacing the hydroxyl oxygen atom with a fluoride (-1 charge) atom and removing the proton, similar to the calculations of Giese (1975). The structures were not minimized after F-for-OH substitution. The F-for-OH substitution decreased the site energy (increased the stability) of the interlayer K site in muscovite (Rothbauer, 1971, structure) from -1246.0 to

-1279.9 kJ/mol. This $\sim 3\%$ decrease in site energy (or increase in stability) reflects the loss of the OH^- dipole. However, this same substitution in phlogopite (Joswig, 1972, structure) changed the K site energy from -949.3 to -1202.9 kJ/mol, a 26.7% decrease in site energy. The same substitution using the Hazen and Burnham (1973) phlogopite structure similarly changed the K site energy from -947.7 to -1201.6 kJ/mol, a 26.8% decrease in site energy. The energetic differences between F-for-OH substitutions in di- and trioctahedral micas result primarily from the electrostatic interaction between the OH^- proton and the interlayer potassium atom. The OH^- dipole is roughly perpendicular to the 2:1 layers in phlogopite, whereas it is tilted toward the vacant octahedral site in muscovite, thereby reducing electrostatic repulsion. The difference in stability gained through F-for-OH substitution is illustrated qualitatively by the differences in these site energies. The thermal results for the hectorite sample suggest that this trioctahedral 2:1 phyllosilicate may decompose thermally in regions within individual crystallites, with hydroxyl-containing domains breaking down before fluoride-containing domains.

Evolution of fluorine from kaolinite

The TGA analyses of the API#9 kaolinite show that the evolution of volatiles from the sample began at $\sim 375^{\circ}\text{C}$, peaked at $\sim 515^{\circ}\text{C}$, and terminated at $\sim 725^{\circ}\text{C}$ (Figure 6). These temperatures represent dehydroxylation of the kaolinite, with the onset of the transformation to metakaolin at $\sim 375^{\circ}\text{C}$ and the final destruction of the

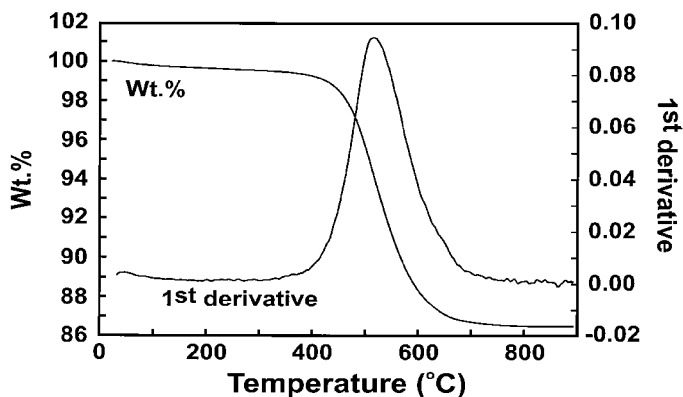


Figure 6. TGA analysis of the API#9 kaolinite. Weight loss is a continuous process between ~ 375 and $\sim 725^\circ\text{C}$ resulting from the dehydroxylation of the kaolinite. Fluoride, although present in this kaolinite, occupies only 0.2% of the hydroxyl sites.

metakaolin structure at $\sim 725^\circ\text{C}$. Chemical analyses of heated aliquots from 16 h step-wise heating of the kaolinite show that fluorine evolved from ~ 400 to $\sim 700^\circ\text{C}$, although a trace of fluorine remained to higher temperatures (Figure 7a).

The thermal reactions were monitored using XRD by measuring the absolute integrated intensity of the 7 Å reflection of kaolinite as the material transformed to metakaolin, yielding a 14 Å peak. The 14 Å peak disappeared as the metakaolin structure broke down to form an amorphous phase at $\sim 725^\circ\text{C}$ (Figure 7b). Fluorine began to evolve from the API#9 kaolinite shortly after the kaolinite transformed to the metakaolin phase. Fluorine evolution terminated at about the same temperature at which evidence for metakaolin disap-

peared, $\sim 725^\circ\text{C}$, which was also the approximate temperature at which dehydroxylation completed.

Unlike smectite, in which the fluorine evolved at higher temperatures than hydroxyl, fluorine evolution in kaolinite coincided with dehydroxylation, suggesting that F-substituted regions gain no stability compared with OH-rich regions. There is no stability gained in kaolinite due to the presence of fluorine. This is in agreement with the electrostatic energy calculations of Wolfe and Giese (1978). They calculated the interlayer bond energies for a theoretical F^- kaolinite in which they replaced OH^- with F. They found that F^- actually creates a slight repulsion between the layers because kaolinite interlayer bonding is dominated by hydrogen bonding; F^- -for- OH^- substitution produces an interlayer with no OH^- dipoles. They

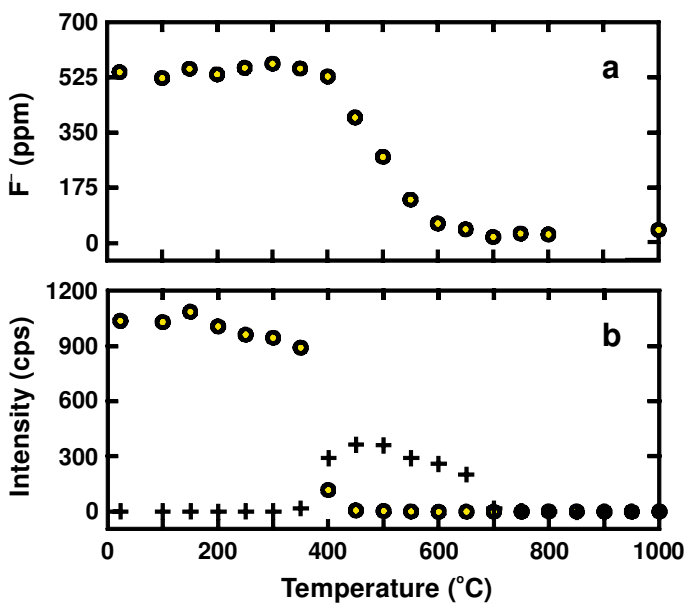


Figure 7. Stepwise 16 h heatings of the API#9 kaolinite. (a) Fluorine content (ppm) as a function of temperature. Fluorine evolution began at $\sim 400^\circ\text{C}$ and terminated at $\sim 700^\circ\text{C}$. (b) Integrated intensity of the 7 Å kaolinite peak (circles) and the broad 14 Å metakaolin peak (crosses) as a function of temperature. Dehydroxylation accompanied by transformation to metakaolin began at $\sim 375^\circ\text{C}$, and final destruction of the metakaolin structure occurred at $\sim 725^\circ\text{C}$.

suggested that an F⁻-kaolinite could exist stably in a fashion similar to that of talc and pyrophyllite, but such a substitution would result in a significantly different manner of layer stacking.

CONCLUSIONS

Our results show that fluorine evolution from the dioctahedral Chew I-S, a raw material used in brick production, occurred at temperatures significantly above the dehydration and dehydroxylation temperatures of the constituent I-S and illite. Interlayer water evolved in two distinct steps, with peaks at ~71 and 136°C, and dehydroxylation occurred between ~350 and 600°C. Fluorine, however, evolved at temperatures between ~600 and 750°C, suggesting that fluoride is significantly stabilized in the smectite structure relative to hydroxyl. Comparison of XRD results for the Chew I-S with the results for F-rich hectorite showed that both clays lost their structural integrity at approximately the same starting and ending temperatures (760–840°C), as shown by the intensities of their 001 reflections. These results show that although fluoride is stabilized in the smectite structure relative to hydroxyl, fluoride does not appear to increase the thermal stability of the smectite structure.

The API#9 kaolinite dehydroxylated between ~375 and 725°C, and fluorine evolution occurred at temperatures from ~400 to 700°C, comparable to dehydroxylation temperatures. It thus appears that fluoride in kaolinite behaves in a manner similar to hydroxyl and is not stabilized in the structure, contrary to the situation with 2:1 layer silicates. This result is consistent with the importance of hydrogen bonding in kaolinite and proton-K interactions in I-S.

These results demonstrate that fluorine evolution will always occur during the firing of clay materials in the brick and tile manufacturing industry if firing temperatures exceed the temperature of structural breakdown. Fluorine emissions cannot be readily reduced by simply varying the temperatures or times used to fire the clay materials. However, fluorine emissions can be minimized through judicious selection of raw materials known to contain less fluorine. They can also be reduced by addition of materials chosen to react selectively with evolving fluorine during processing, e.g. CaCO₃ which breaks down to CaO and combines with F to form CaF₂ (e.g. Kolkmeier 1986; Storer-Folt *et al.*, 1992; Mumenthaler *et al.*, 1995).

ACKNOWLEDGMENTS

We wish to thank D. Counce and P. Trujillo for conducting the fluorine analyses, L. Milam for helpful discussions, and G. Guthrie, R. Giese and an anonymous reviewer for their constructive reviews. We also appreciate the cooperation of the Texas Mining & Reclamation Association.

REFERENCES

- Bassett, W.A. (1960) Role of hydroxyl orientation in mica alteration. *Bulletin of the Geological Society of America*, **71**, 449–456.
- Bish, D.L., Vaniman, D.T. and Chipera, S.J. (1999) Effects of particle size and trace-mineral content on kaolin trace element chemistry. *Proceedings of the 36th Annual Clay Minerals Society Meeting*, p. 15.
- Chipera, S.J. and Bish, D.L. (1989) The nature of fluorine in a partially ordered I/S clay. *Proceedings of the 25th Annual Clay Minerals Society meeting*, p. 23.
- Chipera, S.J., Guthrie, G.D., Jr. and Bish, D.L. (1993) Preparation and Purification of Mineral Dusts. Pp. 235–249 in: *Health Effects of Mineral Dusts* (G.D. Guthrie and B.T. Mossman, editors). Reviews in Mineralogy, **28**. Mineralogical Society of America, Washington, D.C.
- Chung, F.H. (1974) Quantitative interpretation of X-ray diffraction patterns of mixtures. II: Adiabatic principle of X-ray diffraction analysis of mixtures. *Journal of Applied Crystallography*, **7**, 526–531.
- Clarke, F.W. and Washington, H.S. (1924) The composition of the earth's crust. *U.S. Geological Survey Professional Paper* **125**, as referenced in Robinson and Edgington (1946).
- Eagers, R.Y. (1969) *Toxic Properties of Inorganic Fluorine Compounds*. Elsevier, New York, 152 pp.
- Giese, R.F., Jr. (1975) The effect of F/OH substitution on some layer-silicate minerals. *Zeitschrift für Kristallographie*, **141**, 138–144.
- Giese, R.F. (1978) The electrostatic interlayer forces of layer structure minerals. *Clays and Clay Minerals*, **26**, 51–57.
- Giese, R.F., Jr. (1982) Theoretical studies of the kaolin minerals. Electrostatic calculations. *Bulletin de Mineralogie*, **105**, 417–424.
- Hauck, D. and Hilker, E. (1986) Possibilities for the reduction of fluorine emission in the firing of bricks and tiles. *Ziegelindustrie International*, **7-8/86**, 373–385.
- Hazen, R.M. and Burnham, C.W. (1973) The crystal structures of one-layer phlogopite and annite. *American Mineralogist*, **58**, 889–900.
- Ingram, B.L. (1970) Determination of fluoride in silicate rocks without separation of aluminum using a specific ion electrode. *Analytical Chemistry*, **42**, 1825–1827.
- Joswig, W. (1972) Neutronenbeugungsmessungen an einem 1M-phlogopit. *Neues Jahrbuch für Mineralogie-Monatshefte*, 1–11.
- Keller, W.D. (1986) Compositions of condensates from heated clay minerals and shales. *American Mineralogist*, **71**, 1420–1425.
- Kerr, P.F. and Kulp, J.L. (1949) *Reference Clay Localities – United States*. American Petroleum Institute Project **49** (Clay Minerals Standards), Preliminary Report 2, 101 pp.
- Kolkmeier, H. (1986) Emission control in the brick and tile industry. *Ziegelindustrie International*, **10/86**, 516–530.
- Labouriau, A., Kim, Y.-W., Chipera, S.J., Bish, D.L. and Earl, W.L. (1995) A ¹⁹F nuclear magnetic resonance study of natural clays. *Clays and Clay Minerals*, **43**, 697–704.
- Mumenthaler, T., Schmitt, H.W., Peters, T., Ramseyer, K. and Zweili, F. (1995) Tracing the reaction processes during firing of carbonate-containing brick mixes with the help of cathodoluminescence. *Ziegelindustrie International*, **5/95**, 307–318.
- Ohashi, Y. and Burnham, C.W. (1972) Electrostatic and repulsive energies of the M1 and M2 cation sites in pyroxenes. *Journal of Geophysical Research*, **77**, 5761–5766.
- Reynolds, R.C., Jr. and Reynolds, R.C., III (1987) *Description of program NEWMOD for the calculation of the one-*

- dimensional X-ray diffraction patterns of mixed-layered clays*. Department of Earth Sciences, Dartmouth College, Hanover, New Hampshire.
- Robinson, W.O. and Edgington, G. (1946) Fluorine in soils. *Soil Science*, **61**, 341–353.
- Romo, L.A. and Roy, R. (1957) Studies of the substitution of OH⁻ by F⁻ in various hydroxylic minerals. *American Mineralogist*, **42**, 165–177.
- Rothbauer, R. (1971) Untersuchung eines 2M₁-muskovits mit neutronenstrahlen. *Neues Jahrbuch für Mineralogie-Monatshefte*, 143–154.
- Sedej, B. (1988) The emission of volatile fluorides during the process in the ceramic industry. *Ziegelindustrie International*, **7-8/88**, 372–376.
- Steinkoenig, L.A. (1919) The relation of fluorine in soils, plants, and animals. *Journal of Industrial and Engineering Chemistry*, **11**, 463, as referenced in Robinson and Edgington (1946).
- Storer-Folt, J.A., Cooper, D.J. and Boeck, E. (1992) Fluorine release in a brick tunnel kiln. *Ceramic Bulletin*, **71**, 636–638.
- Strohmeier, W. (1983) Problems associated with fluorine. *Ziegelindustrie International*, **2/83**, 67–72.
- Sugiyama, H., Ōya, A. and Ōtani, S. (1988) Syntheses and thermal degradation behaviours of saponite- α -naphthylamine complexes: Effects of substitution of OH in saponite by fluorine. *Journal of Materials Science*, **23**, 1764–1768.
- Thomas, J., Jr., Glass, H.D., White, W.A. and Trandel, R.M. (1977) Fluorine content of clay minerals and argillaceous earth materials. *Clays and Clay Minerals*, **25**, 278–284.
- Troll, G., Farzaneh, A. and Cammann, K. (1977) Rapid determination of fluoride in mineral and rock samples using an ion-selective electrode. *Chemical Geology*, **20**, 295–305.
- Wilson, H.H. and Johnson, L.D. (1975) Characterization of air pollutants emitted from brick plant kilns. *Ceramic Bulletin*, **54**, 990–993.
- Wolfe, R.W. and Giese, R.F., Jr. (1978) The stability of fluorine analogues of kaolinite. *Clays and Clay Minerals*, **26**, 76–78.

(Received 17 November 2000; revised 8 May 2001; Ms. 502)